Appl Biochem Biotechnol (2017) 182:721–741
DOI 10.1007/s12010-016-2357-4

Cloning, Characterization, and Expression Analysis of a Gene Encoding a Putative Lysophosphatidic Acid Acyltransferase from Seeds of *Paeonia rockii*

Qing-Yu Zhang[1] · Li-Xin Niu[1] · Rui Yu[1] · Xiao-Xiao Zhang[1] · Zhang-Zhen Bai[1] · Ke Duan[2] · Qing-Hua Gao[2] · Yan-Long Zhang[1]

Received: 18 August 2016 / Accepted: 5 December 2016 /
Published online: 16 December 2016

Abstract Tree peony (*Paeonia* section *Moutan* DC.) is an excellent woody oil crop, and the cloning and functional analysis of genes related to fatty acid (FA) metabolism from this organism has not been reported. Lysophosphatidic acid acyltransferase (LPAAT), which

Electronic supplementary material The online version of this article (doi:10.1007/s12010-016-2357-4) contains supplementary material, which is available to authorized users.

✉ Yan-Long Zhang
zhangyanlong@nwsuaf.edu.cn

Qing-Yu Zhang
zhangqingyu@nwsuaf.edu.cn

Li-Xin Niu
niulixin@nwsuaf.edu.cn

Rui Yu
yurui@nwsuaf.edu.cn

Xiao-Xiao Zhang
zhangxiaoxiao@nwsuaf.edu.cn

Zhang-Zhen Bai
baizhangzhen@nwsuaf.edu.cn

Ke Duan
duanke@saas.sh.cn

Qing-Hua Gao
gaoqinghua@saas.sh.cn

[1] College of Landscape Architecture and Arts, Northwest A&F University, Yangling, Shaanxi 712100, China

[2] Shanghai Key Laboratory of Protected Horticultural Technology, Forestry and Fruit Tree Research Institute, Shanghai Academy of Agricultural Sciences (SAAS), Shanghai 201403, China

converts lysophosphatidic acid (LPA) to phosphatidic acid (PA), catalyzes the addition of fatty acyl moieties to the sn-2 position of the LPA glycerol backbone in triacylglycerol (TAG) biosynthesis. This project reports a putative lysophosphatidic acid acyltransferase gene *PrLPAAT1* isolated from *Paeonia rockii*. Our data indicated that *PrLPAAT1* has 1047 nucleotides and encodes a putative 38.8 kDa protein with 348 amino acid residues. Bioinformatic analysis demonstrated that *PrLPAAT1* contains two transmembrane domains (TMDs). Subcellular localization analysis confirmed that PrLPAAT1 is a plasma membrane protein. Phylogenetic analysis revealed that PrLPAAT1 shared 74.3 and 65.5% amino acid sequence identities with the LPAAT1 sequences from columbine and grape, respectively. PrLPAAT1 belongs to AGPAT family, and may have acyltransferase activity. *PrLPAAT1* was ubiquitously expressed in diverse tissues, and *PrLPAAT1* expression was higher in the flower and developing seed. *PrLPAAT1* is probably an important component in the FA accumulation process, especially during the early stages of seed development. *PrLPAAT1* overexpression using a seed-specific promoter increased total FA content and the main FA accumulation in Arabidopsis transgenic plants.

Keywords Gene cloning · Expression profile · Lysophosphatidic acid acyltransferase · *Paeonia rockii* · Structure and function

Introduction

Tree peony is a new woody oil crop that has a high oil production rate and good oil quality. It belongs to section *Moutan* of the genus *Paeonia* in the family Paeoniaceae, and all 9 wild species are endemic to China [1, 2]. Tree peony's follicle has a star-shaped fruit. It contains black oval seeds that are characterized by abundant UFAs (>90% of the total FA content) and a high proportion of n-3 FAs (ALA, >40% of the total FA content) that can markedly improve the structure of diet and human health [3, 4]. As an alternative source of edible oil, the tree peony could be sustainably exploited and be a good model for dissecting the metabolic pathways involved in seed oil synthesis. According to previous reports, there are more than 20,267 ha of the cultivated area of the tree peony in China, which have a potential annual seed production of 57,855 tons [5].

As a major storage lipid, triacylglycerol (TAG) could be accumulated in seeds or fruits as well as other tissues, such as flower petals, senescing leaves and pollen grains in higher plants [6–8]. Plant-derived TAG is an important renewable source of reduced carbon that can be used as food, biofuel and industrial feedstock [9–11]. Through the conventional Kennedy pathway in the endoplasmic reticulum (ER), TAG is synthesized de novo in three acylation reactions at the sn-1-, sn-2-, and sn-3-positions of the glycerol-3-phosphate (G3P) backbone with acyl chains from acyl-CoAs, and these three reactions respectively are catalyzed by glycerol-3-phosphate acyltransferase (GPAT), LPAAT, and diacylglycerol acyltransferase (DGAT) [12, 13]. The acyl-CoAs can also be incorporated into PC by the acyl editing reactions besides Kennedy pathway [14]. In fact, by transacylation of the sn-2 FA from PC onto sn-3 position of DAG, Phospholipid:DAG acyltransferase (PDAT) could be used to syntheses TAG [15, 16].

LPAAT could catalyze LPA to yield PA by acylation of the sn-2 position of G3P. In animals, this enzyme is also named as acyl-CoA:1-acylglycerol-sn-3-phosphate acyltransferase (AGPAT) [17–19]. LPAAT enzymes have been associated with multiple membrane

systems in plants, including the mitochondrial outer membrane, endoplasmic reticulum (ER), and chloroplasts. Besides, LPAAT is able to discriminate acyl groups with different chain lengths and possesses a selectivity and specificity for unsaturated C18 acyl groups in traditional oil seed crops [19]. Several studies performed on different plant species have revealed the presence of at least two gene classes (class A and class B) that encode microsomal LPAATs. There are five isolated and annotated *LPAAT* genes designated *AtLPAAT1–5* in the Arabidopsis genome [20]. These genes include the plastidial isoenzyme gene (*AtLPAAT1*), two class-A related genes, *AtLPAAT2* and *AtLPAAT3*, a gene encoding an anther specific isoenzyme, and two less related members, *AtLPAAT4* and *AtLPAAT5*, which encode proteins without detectable LPAAT activity in vitro that seem to be related to cardiolipin biosynthetic enzymes. No representative of the class-B is found in the Arabidopsis genome [20–22]. The so-called class-B LPAATs were first cloned and characterized from *Limnanthes douglasii* [23, 24] and *Cocos nucifera* [25]. More recently, this gene was also identified in *Ricinus communis* [22]. The *LPAATB* has a substrate preference for unusual acyl groups and could be typically expressed in seeds. Interestingly, the *LPAAT2* gene of class A also can acylate unusual fatty acids into sn-2 TAG [26, 27].

Recent results suggest that *LPAATs* also play important roles in TAG accumulation. Overexpression of *B. napus* microsomal LPAAT isozymes enhanced the TAG accumulation and lipid content in Arabidopsis seeds [28]. Seed-specific overexpression of *AhLPAAT2* (from Peanut) in Arabidopsis resulted in a greater-than-average seed weight and higher seed oil content. The proportion of unsaturated FAs and total FA content also increased in this study [13]. When microsomal *LPAAT* genes (*BAT1.13* and *BAT1.5*, which encode rapeseed microsomal LPAATs) from rapeseed were overexpressed in Arabidopsis in a seed-specific manner, the average seed weight and the total fatty acid content of seed storage lipids increased by 6 and 13%, respectively, compared with those of nontransformed plants [28, 29]. When the yeast genes *SLC1* and *SLC1–1* (homologs of ER-localized *LPAATs* in Arabidopsis) were overexpressed in soybean, rapeseed, and Arabidopsis, the seed TAG content increased [30, 31]. Therefore, *LPAAT* could be a potential valuable gene for increasing TAG accumulation.

The plastid-located *LPAAT1* is participated in the production of PA with C16 FAs, which is similar to the prokaryotic form [19], notably LPAAT1 which displays substrate preference for 16:0 over 18:1 CoA [32]. LPAAT1 is required for operation of the prokaryotic pathway that produces monogalactosyldiacylglycerol (MGD), digalactosyldiacylglycerol (DGD), phosphatidylglycerol (PG), and sulfoquinovosyldiacylglycerol (SQD) for thylakoid biogenesis [33]. Lipidomic analysis indicated that the deletion of *Metarhizium robertsii mrLPAAT1* (LPAAT activity was similar to yeast *SLC1*) resulted in significant increases in TAG, FAs, and phosphatidylcholine (PC) but decreased PA, phosphatidylethanolamine (PE), and other species of phospholipids when compared to the wild type [34]. So it is reasonable to conclude that LPAAT1 is essential for synthesis of FAs and lipids in eucaryon.

In this study, we isolated and sequenced a *PrLPAAT1* gene from the tree peony and analyzed its putative structure-function relationships. The expression profile *PrLPAAT1* was investigated in different organs as well as in seeds at different developmental stages. The subcellular localization of *PrLPAAT1* was examined. Moreover, we measured the FA content of mature seeds in *PrLPAAT1* transgenic Arabidopsis lines by GC-MS. Our results will facilitate understanding of the biochemical role that *PrLPAAT1* plays in the tree peony.

Materials and Methods

Plant Material and Treatments

A wild relative of tree peony *Paeonia rockii* with high oil content and α-linolenic acid content grown in Wild Tree Peony Germplasm Repository at Northwest A&F University (Yangling, China) was used in this study. Seven organs including the root, stem, leaf, calyx, petal, stamen, pistil, and developing seeds (20, 30, 40, 50, 60, 70, 80, 90, and 100 days after flowering, or DAF) were used for gene expression analysis. Each experiment was repeated three times in which at least two plants were bulked. All samples were immediately frozen in liquid nitrogen and stored at −80 °C before DNA and RNA extraction. The seeds from different developmental stages were naturally dried and stored in a brown dryer which filled with nitrogen more than 48 h for fatty acid composition analysis.

Seed Oil Content Measurement by GC-MS

The FAs of tree peony seeds were extracted, and fatty acid methylation was completed according to procedures described in a previous study [5]. FA was analyzed by using a gas chromatograph-mass spectrometer (GC7890A/MS5975C, Agilent Technologies, Santa Clara, CA) equipped with a G4513A autosampler (Agilent). The column was HP-88 (100 m × 0.25 mm i.d., 0.20-μm film thickness; Agilent). As the quantitative approach, an internal standard curve method was used to construct five calibration plots of analyte/internal standard peak-area ratio versus standard concentration which was determined by the least squares method. The methyl heptadecanoate was used as the internal standard and the FAMEs were measured in each sample. The FAMEs of samples were recorded as milligrams per gram dry weight (DW). All samples were analyzed in triplicate.

Genomic DNA and Total RNA Extraction

Genomic DNA was extracted from 30 DAF seeds of the tree peony using the hexadecyltrimethylammonium bromide (CTAB) method as described previously [35]. Total plant RNA was extracted using the TIANGEN RNA Prep Pure Plant kit (Tiangen Biotech Co. Ltd., Beijing, China) following the manufacturer's instructions. The concentration and quality of RNA samples were inspected by spectrophotometric analysis and Goldview-stained agarose gel electrophoresis. Total RNA samples were treated 2 min at 42 °C for removing genomic DNA contamination. The first-strand cDNAs were synthesized at 37 °C for 15 min followed by 85 °C for 5 s by using PrimeScript® RT reagent Kit with gDNA Eraser (DRR047A, Takara, Dalian, China).

Cloning of Full-Length *PrLPAAT1* cDNA and Genomic DNA

Two pairs of degenerate primers composed of two sense primers and one antisense primer (Table 1) directed against the 1-acyl-sn-glycerol-3-phosphate acyltransferase-related domain were used to amplify the conserved regions of the tree peony *LPAAT1* gene with cDNA templates from 30 DAF seeds. Based on the partial cDNA clones for tree peony *LPAAT1*, the full-length cDNA was amplified by rapid amplification of cDNA ends (RACE). The 5′ cDNA ends and 3′ cDNA ends were isolated following the SMARTer® RACE 5′/3′ Kit User Manual (Clontech Laboratories, Inc., USA). To amplify full-length clones from cDNA or DNA templates, primers (in

Table 1 Primers used in this study

Name	Primer sequences (5′- 3′)	Application
dp-S1	RYTSCTGCTGTRTATGTKTC	Degenerated primers for amplification of the conserved region[a]
dp-S2	WYAAGTTYATYAGCAAGAC	
dp-A1	CCATCYTTRCTSCGWGTTC	
LPAAT1–1F3(GSP1)	GATTACGCCAAGCTTTTAAGTTTATTAGCAAGAC	3'RACE
LPAAT1-2F3(NGSP1)	GATTACGCCAAGCTTCAGCAGAAGCCAGTTGGAG	
LPAAT1–1R5(GSP1)	GATTACGCCAAGCTTCCATCTTTACTCCGTGTTCCC	5'RACE
LPAAT1-2R5(NGSP1)	GATTACGCCAAGCTTTCCAACTGGCTTCTGCTGTCC	
LPAAT1F	TCTTCGGATTGCCACATTTCG	Full-length cDNA PCR
LPAAT1R	GTTAGCCTTGAGAATTGAGCG	
LPAAT1F	TCTTCGGATTGCCACATTTCG	Full-length DNA PCR
LPAAT1R	GTTAGCCTTGAGAATTGAGCG	
LPAAT1RT-F	ACAGCAGAAGCCAGTTGGAG	RT-PCR
LPAAT1RT-R	CGCAGGCATTATTTGTCCCG	

Table 1) spanning full open reading frames (ORFs) were designed. All amplicons were connected into the pUCm-T vector (SK2212, Sangon, Shanghai, China) for sequencing.

Bioinformatic Analysis

Genomic DNA and cDNA alignments as well as splice signal identification were performed using NCBI Splign (http://www.ncbi.nlm.nih.gov/sutils/splign/). Conserved domain analysis was carried out using Conserved Domain Databases (NCBI CDD). The PrLPAAT1 active sites were predicted by PROSITE in Predictprotein (http://www.predictprotein.org/). The hydrophobicity profile and charge density distribution of PrLPAAT1 were predicted using ExPASy (http://www.expasy.org/), the secondary structure of PrLPAAT1 was predicted using SOPMA (https://npsa-prabi.ibcp.fr/cgi-bin/npsa_automat.pl?page=/NPSA/npsa_sopma.html). The putative subcellular localization was estimated by PSORT Prediction (http://psort.hgc.jp/form.html). PrLPAAT1 tertiary structural model was constructed using the Phyre Version 0.2 [36]. Alignments of LPAAT1 protein sequences were achieved using ClustalW1.83 [37] with the default settings. The alignment output was used to generate a cladogram based on the neighbor-joining method [38], as implemented in the MEGA 5.0 [39]. The sizes of exon and intron from the selected *LPAAT1* genes were estimated, and the structural models of gene and protein were drawn with FancyGENE v1.4 [40]. Based on the complete protein sequences, the transmembrane domains (TMDs) of LPAAT1 were predicted by the SMART database (http://smart.emblheidelberg.de/) and the transmembrane prediction server TMHMM-2.0 (http://www.cbs.dtu.dk/services/).

Protein Subcellular Localization Analysis

The *PrLPAAT1* ORF without the stop codon was inserted into the *BamH* I–*Sal* I sites of pC1301-GFP vector, generating a construct with GFP at the C-terminal of *PrLPAAT1* under

the control of the 35S promoter from cauliflower mosaic virus (CaMV). This construct was transferred into the Agrobacterium engineering strain EHA105 by microprojectile bombardment, and the transfectants were streaked onto a YEB plate containing 50 mg/mL Kan and Rif to obtain single colonies at 28 °C in dark by inverted culture. Single colonies were picked on the transformation plates and inoculated into 1 mL YEB liquid medium containing the same antibiotics at 220 rpm and 28 °C with shaking overnight. One milliliter of the above culture was added to 50 mL YEB liquid medium containing the same antibiotic and incubated and shook at 220 rpm at 28 °C for approximately 10 h to obtain 0.3 of OD600. The culture was centrifuged at 5000 rpm for 15 min in room temperature, the supernatant was discarded, and the cells were suspended in the same volume of infiltration buffer (10 mM MES, 200 μM acetosyringone, and 10 mM $MgCl_2$, pH 5.6), incubated for 4 h at room temperature, and then delivered into the lower epidermis of 4-week-old tobacco leaves. The cells were imaged 4–6 days after transfection using an UltraVIEW Vox spinning disk confocal system (PerkinElmer, Cambridge, UK).

Gene Expression Analysis

Quantitative real-time RT-PCR was performed on a LightCycler480 Real-Time PCR System (Roche Diagnostics, Basel, Switzerland) with a Premix Ex Taq™ (Perfect Real Time) kit (DRR041A, Takara, Dalian, China). The PCR conditions were set as follows: 95 °C for 15 s followed by 45 cycles of 95 °C for 5 s, 58 °C for 30 s, and 72 °C for 31 s. Fluorescence data which were collected during the 72 °C step were analyzed with LightCycler480 analysis software. In qRT-PCR analysis, the relative expression of genes were estimated by $2^{-\Delta\Delta CT}$. The interspacer 26S–18S tree peony RNA gene was used as the housekeeping gene (forword primer: 5′-ACCGTTGATTCGCACAATTGGTCATCG-3′ and reverse primer: 5′-TACT GCGGGTCGGC AATCGGACG-3′). The primers of genes for RT-PCR are provided in Table 1. All reactions were conducted in triplicate in one experiment, and three biological replicates were carried out.

Arabidopsis thaliana Transformation

The construct harboring 2S2:*PrLPAAT1* was transformed into wild type Arabidopsis plants using a floral-dip method [41]. The seeds of transgenic plants were selected on 1/2 MS medium containing 20 mg L^{-1} hygromycin (Hyg). The Arabidopsis plants were sealed with parafilm and cultivated in Sanyo MLR 351H growth chamber, with a 120 μmol m^{-2} s^{-1} photo flux density and 14-h light/10-h dark cycle, at 22 ± 2 °C for 10 days before transplanting to soil. The FAs content of mature Arabidopsis seeds were measured as described previously [28].

Results

Cloning and Nucleotide Sequence Analysis of *PrLPAAT1*

The cDNA fragments (190 bp) spanning the conserved region of *LPAAT*-type genes were isolated from 30 DAF seeds. Based on the partial cDNA clones, the full-length cDNA (1047 bp) and DNA (1047 bp) clones were carried out by RACE experiments. With this information, we concluded that *PrLPAAT1* does not contain introns. The full-length cDNA

fragment harboring a 1047 bp ORF and encoding a 348-aa peptide was named *PrLPAAT1*. This gene was deposited into GenBank (the accession number: KX256278). The ORF of the *PrLPAAT1* gene encoded a protein of 348 amino acid residues with a calculated molecular mass of 38.8 kDa and an isoelectric point of 9.68. Conserved domain analysis detected a conserved 1-acyl-sn-glycerol-3-phosphate acyltransferase-related (PLN02901) and LPLAT_AGPAT-like (cd07989) domain (Fig. 1a).

The sequence alignment of PrLPAAT1, AGPATs, and LPAATs shown that the acyltransferase motifs I, III, and IV were discovered and they have strong homology (Fig. 1b). Among AGPAT family, the acyltransferase motif I and motif III are the most conserved regions, all proteins possess the HXXXXD signature and most of them possess the PEGT-X signature; motif IV is less conserved, however, it is rich in hydrophobic amino acids [42, 43]. Previous studies have reported that the HXXXXD signature from motif I is important for the acyltransferase activity [44], motif III is participated in binding of the acyl acceptor [42], and motif IV may be involved in acyl-CoA binding [45]. Therefore, we proposed that PrLPAAT1 may be a member of AGPAT family, and may have acyltransferase activity. Moreover, motif II is also participated in binding of the acyl acceptor [46], but it is not found in PrLPAAT1.

The Predicted Structure of the PrLPAAT1 Protein

Hydrophobicity prediction using the Kyte-Doolittle algorithm revealed more hydrophobic residues (188 amino acids) than hydrophilic residues (160 amino acids), suggesting that PrLPAAT1 was a hydrophobic protein. Two strongly hydrophobic stretches with approximately 30 amino acids were separately distributed in N- and C-terminal regions (Fig. 2a). Secondary structure prediction demonstrated that the putative PrLPAAT1 protein contained 28.74% α-helices (12 helices total), 21.84% extended strands (19 strands total), 9.20% β-turns (11 turns total), and 40.23% random coils (Fig. 2b). In addition, PSORT II predicted that this

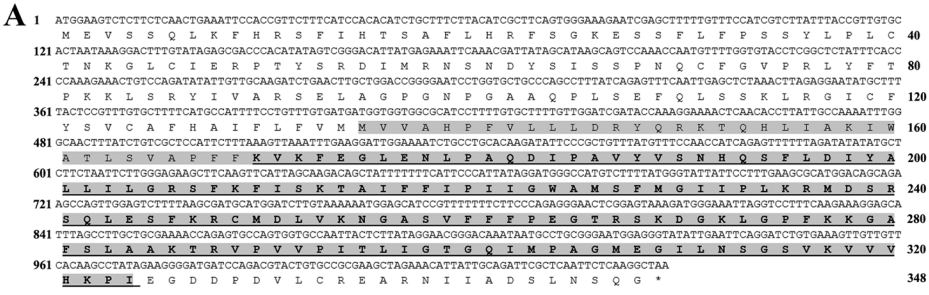

Fig. 1 **a** Nucleotide and deduced amino acid sequence of *PrLPAAT1* cDNA from the tree peony. The *residues with gray backgrounds* indicate the conserved 1-acylglycerol-3-phosphate acyltransferase-related domain. The *underlined bold letters in gray background* indicate a LPLAT_AGPAT-like domain. **b** Acyltransferase motifs in PrLPAAT1, AGPATs, and LPAATs. The conserved amino acid residues are shown in *color*

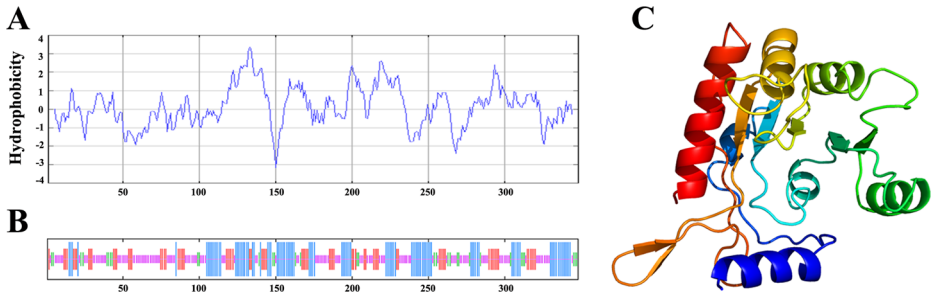

Fig. 2 The predicted structure of the PrLPAAT1 protein. **a** Hydrophobicity plot predicted by the Kyte-Doolittle method of a sliding window average over nine neighboring residues. **b** The secondary structure of PrLPAAT1. *Blue long lines* show the predicted α-helices, *short red lines* the extended strands, *green short lines* the β-turns, and *pink short lines* the random coils. **c** Tertiary structure characteristics of the partial PrLPAAT1 protein. The *helical structures* show the predicted α-helices, and the *flat arrows* indicate the β-sheets

protein was located on the mitochondrial inner membrane and the plasma membrane. Further prediction of PrLPAAT1 transmembrane topology using TMHMM-2.0 revealed that PrLPAAT1 contained tswo TMDs (Fig. 4b). Phyre homology modeling of PrLPAAT1 showed a folding mode and spatial configuration similar to that of MsPatA (PDB code 5F34) [47] and CmGPAT (PDB code 1IUQ) [48]. The stereo diagrams indicated that the secondary structure elements of PrLPAAT1 were organized into a compact domain consisting seven α-helices and eight β-sheets (Fig. 2c).

Phylogenetic Relationships of the *LPAAT1* Genes in Eukaryotes

To better understand the relationships between the tree peony *LPAAT1* gene and those of other eukaryotes (animals, plants, and algae), we explored the evolutionary histories of *LPAAT1* genes by using full-length sequences to construct phylogenetic trees. A compact view of the tree is shown in Fig. 3 based on the LPLAT_AGPAT-like domain. Our phylogenetic analyses indicated that the possible evolutionary relationships of the *LPAAT1* genes could be predicted via homology searches. Homologs of the plastidic *LPAAT1* genes were discovered in all species (except the plant *Setaria italica*) with sequenced genomes. All plant species harbored a single *LPAAT1* gene but the *G. max* which possessed four copies of *LPAAT1* [19]. The results of cloning showed that *Paeonia rockii* harbored a single *LPAAT1* gene.

As shown in Fig. 3, all plant *LPAAT1* homologs grouped in a cluster. Interestingly, the green algae *Physcomitrella patens*, *Coccomyxa subellipsoidea*, *Chlamydomonas reinhardtii*, *Micromonas pusilla*, and *Ostreococcus lucimarinus* presented a single *LPAAT1* gene and grouped in a cluster together with plant *LPAAT1* (Fig. 3). All animal *LPAAT1* homologs grouped into another cluster. *AGPAT1* and *AGPAT2* are paralogous genes in metazoan species, which originated from a duplication event. With the exception of the fish *Danio rerio*, homologs of the *AGPAT1* and *AGPAT2* genes were found in almost all of animal species studied. Although the human *AGPAT1* and *AGPAT2* genes encode respective proteins which have nonredundant functions, they have quite similar biochemical properties [49]. The results indicated that tree peony *LPAAT1* appeared to be more closely related to *AcLPAAT1* (from *Aquilegia coerulea*) than other *LPAAT1* isoforms, suggesting that tree peony and columbine *LPAAT1* had a common origin. PrLPAAT1 shared 74.3 and 65.5% amino acid sequence identities with those from columbine and grape, respectively.

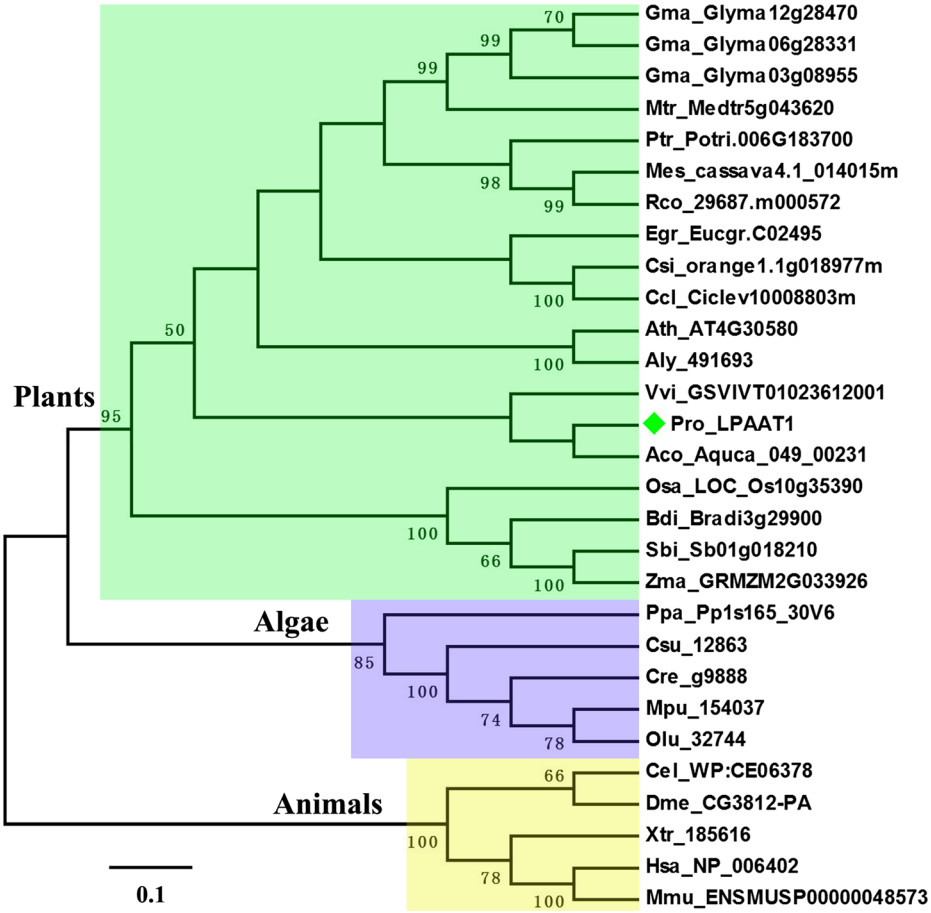

Fig. 3 Phylogenetic analysis of the selected LPAAT1 members. The percentage of replicate trees in which the associated taxa clustered together in the bootstrap test (1000 replicates) is shown at each node. The *scale bar* represents the number of substitutions per amino acid site. The clusters or subclusters grouping each LPAAT1 are highlighted with *different colors* in the figure: plants (*green*), algae (*purple*), and animals (*yellow*). The complete list of species is presented in Table 2

Comparative Analysis of Gene Structure and Conserved Domains in LPAAT1 Protein

To better understand the evolutionary rules of *LPAAT1* structural organization, protein function among species, the gene structure of *LPAAT1* was explored in eukaryotes [50]. The cDNA sequences were aligned with their corresponding genomic DNA sequences, subsequently, the exons and intron lengths of *LPAAT1* were manually counted. In clusters of each isoform of *LPAAT1*, the gene structure was relatively conserved, however, the number of introns was fairly different in plants and animals (Fig. 4a and Table 2). In the cluster of the representative plants, there were six introns within the Arabidopsis *LPAAT1* gene, whereas only four introns in the rice *LPAAT1* gene (Fig. 4a). Nevertheless, the *LPAAT1* genes within the cluster of representative plants have high conservation in exon size, especially in the middle portion of the genes. Interestingly, the tree peony *LPAAT1* gene did not contain any intron sequences

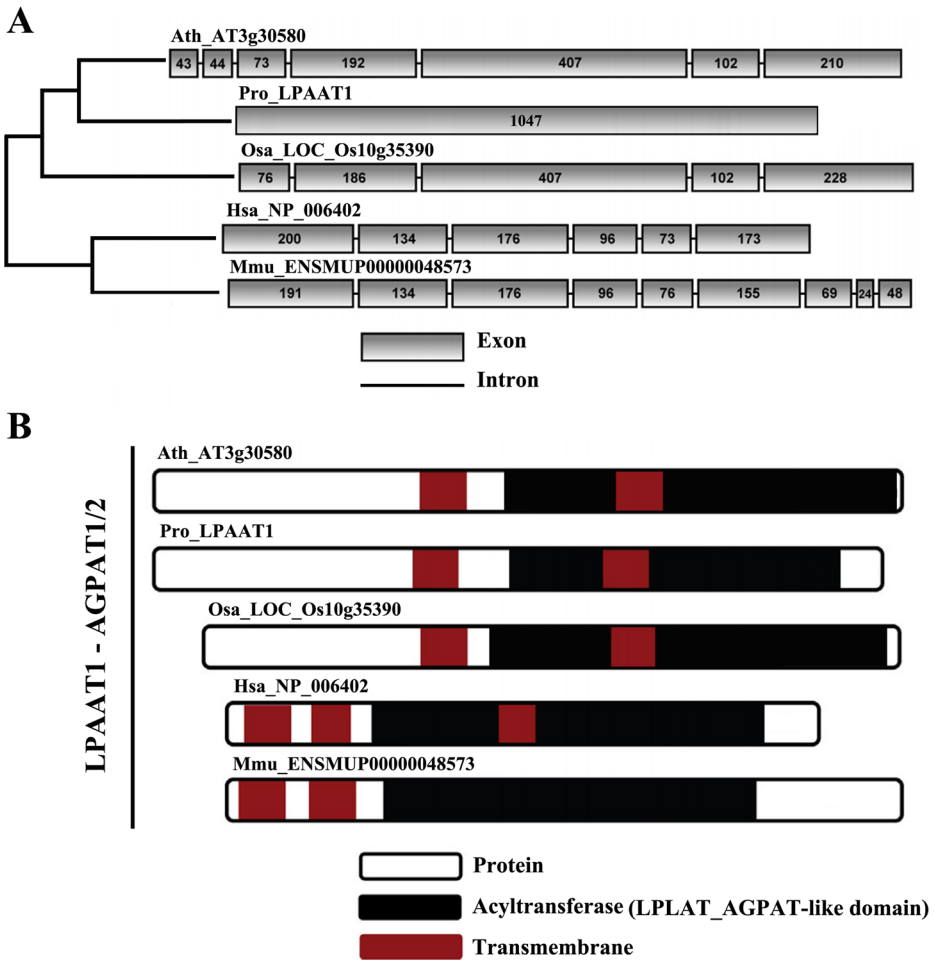

Fig. 4 Comparative analysis of gene structure and conserved domains in the LPAAT1 protein. **a** Exon-intron structure of plant and animal *LPAAT1* genes. Representative sequences of eudicots, monocots, and animals are presented for each cluster: *A. thaliana* (Ath), *O. sativa* (Osa), *P. rockii* (Pro), *M. musculus* (Mmu) and *H. sapiens* (Hsa). The size of each exon is shown in bp. **b** Prediction of the transmembrane and acyltransferase domains of plant and metazoan LPAAT1 proteins. Predicted transmembrane structures (*red*) and LPLAT_AGPAT-like domain (*black*) of representative species were obtained using the transmembrane prediction server TMHMM-2.0 and the SMART database with the complete protein sequences. The sequences are represented as *simplified boxes*. The size of each sequence is shown in amino acid residues (aa)

(Fig. 4a), which is very rare in eukaryote *LPAAT1* genes. Between human *AGPAT1/2* and mouse *AGPAT1/2*, we could observe a higher conservation of exon sizes and mild variation in the number of introns (Fig. 4a).

As we see, the amino acid length of the LPAAT1s ranged from 214 to 423 residues (Table 2). We explored the conserved domains and analyzed the functional motifs in the representative proteins of plant and animal species which have been depicted in Fig. 4b. Predictions of transmembrane (TrM) structures suggested that each *LPAAT1* gene at least have two regions which contained an extremely probable TrM sequence (Fig. 4b), the above shown that the LPAAT1 proteins are membrane-associated. As depicted in Fig. 4b for the protein

Table 2 Sequences retrieved

Family	Specie	Taxa	Gene	Protein ID	Length (aa)	No. Introns	Database
Euphorbiaceae	*Manihot esculenta*	Mes	LPAAT1	cassava4.1_014015m	266	5	Phytozome
Euphorbiaceae	*Ricinus communis*	Rco	LPAAT1	29,687.m000572	303	4	Phytozome
Salicaceae	*Populus trichocarpa*	Ptr	LPAAT1	Potri.006G183700	363	6	Phytozome
Fabaceae	*Medicago truncatula*	Mtr	LPAAT1	Medtr5g043620	333	3	Phytozome
Fabaceae	*Glycine max*	Gma	LPAAT1	Glyma12g28470	355	6	Phytozome
Fabaceae	*Glycine max*	Gma	LPAAT1	Glyma06g28331	345	6	Phytozome
Fabaceae	*Glycine max*	Gma	LPAAT1	Glyma03g08955	230	2	Phytozome
Brassicacea	*Arabidopsis thaliana*	Ath	LPAAT1 (ATS2)	AT4G30580	356	6	Phytozome
Brassicacea	*Arabidopsis lyrata*	Aly	LPAAT1	491,693	358	6	Phytozome
Rutaceae	*Citrus sinensis*	Csi	LPAAT1	orange1.1g018977m	348	6	Phytozome
Rutaceae	*Citrus clementina*	Ccl	LPAAT1	Ciclev10008803m	348	6	Phytozome
Myrtaceae	*Eucalyptus grandis*	Egr	LPAAT1	Eucgr.C02495	369	6	Phytozome
Vitaceae	*Vitis vinifera*	Vvi	LPAAT1	GSVIVT01023612001	423	6	Phytozome
Ranunculaceae	*Aquilegia coerulea Goldsmith*	Aco	LPAAT1	Aquca_049_00231	340	4	Phytozome
Poaceae	*Sorghum bicolor*	Sbi	LPAAT1	Sb01g018210	330	4	Phytozome
Poaceae	*Zea mays*	Zma	LPAAT1	GRMZM2G033926	334	4	Phytozome
Poaceae	*Oryza sativa*	Osa	LPAAT1	LOC_Os10g35390	332	4	Phytozome
Poaceae	*Brachypodium distachyon*	Bdi	LPAAT1	Bradi3g29900	332	4	Phytozome
Funariaceae	*Physcomitrella patens*	Ppa	LPAAT1	Pp1s165_30V6	372	5	Phytozome
Chlamydomonadaceae	*Chlamydomonas reinhardtii*	Cre	LPAAT1	g9888	332	7	Phytozome
Coccomyxaceae	*Coccomyxa subellipsoidea C-169*	Csu	LPAAT1	12,863	232	ND	Phytozome
Mamiellaceae	*Micromonas pusilla CCMP1545*	Mpu	LPAAT1	154,037	214	ND	Phytozome

Table 2 (continued)

Family	Specie	Taxa	Gene	Protein ID	Length (aa)	No. Introns	Database
Mamiellaceae	*Ostreococcus lucimarinus*	Olu	LPAAT1	32,744	214	ND	Phytozome
Rhabditidae	*Caenorhabditis elegans*	Cel	AGPAT1/2	WP:CE06378	282	4	Metazome
Drosophilidae	*Drosophila melanogaster*	Dme	AGPAT1/2	CG3812-PA	343	2	Metazome
Pipidae	*Xenopus tropicalis*	Xtr	AGPAT1	185,616	273	7	Metazome
Hominidae	*Homo sapiens*	Hsa	AGPAT1	NP_006402	283	5	NCBI
Muridae	*Mus musculus*	Mmu	AGPAT1	ENSMUSP00000048573	322	8	Metazome

sequences of the representative species, the acyltransferase (LPLAT_AGPAT-like) domain could also been observed in all of the LPAAT1 proteins. Interestingly, it is shown that proteins within the cluster plants normally presented one TrM structure overlapping the LPLAT_AGPAT-like domain, which was also observed in the tree peony LPAAT1 protein.

Subcellular Localization of the PrLPAAT1 Protein

To determine the subcellular localization of the PrLPAAT1 protein, the fusion protein expression vector 35S::PrLPAAT1-GFP (pC1301-PrLPAAT1-GFP) was transformed into the lower epidermis of tobacco by Agrobacterium-mediated transformation method using an empty vector 35S::GFP (pC1301-GFP) as a control. The results showed that the green fluorescence of tobacco lower epidermal cells transformed with the control 35S::GFP was spread throughout the entire cellular structure, including the cytomembrane, cytoplasm and nucleus (Fig. 5). In contrast, the green fluorescence of the 35S::PrLPAAT1-GFP chimera was located at the plasma membrane in the tobacco lower epidermal cells (Fig. 5), and these results indicated that PrLPAAT1 was a plasma membrane protein, which was consistent with the subcellular localization prediction results.

Expression Pattern of the *PrLPAAT1* Gene

The expression of *PrLPAAT1* in different tree peony organs was determined using qRT-PCR. The results showed that *PrLPAAT1* was constitutively expressed in the tree peony, with higher

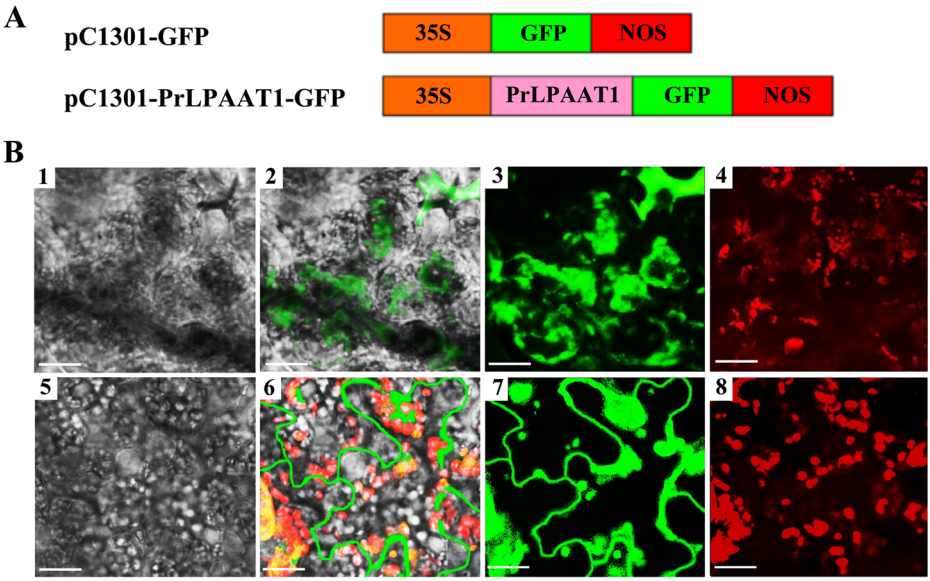

Fig. 5 Subcellular localization of PrLPAAT1–GFP fusion protein in the transgenic tobacco cells. **a** Schematic diagram of the construction of the recombinant PrLPAAT1-GFP vector. 35S: a constitutive promoter from the cauliflower mosaic virus; GFP: green fluorescent protein; NOS: nopaline synthase terminator. **b** 1–4: Transgenic plant pC1301-GFP florescent detection; 5–8: Transgenic plants pC1301-PrLPAAT1-GFP florescent detection; 1, 5 are bright field images; 3, 7 are GFP florescence; 4, 8 are Chlorophyll autofluorescence; 2, 6 are overlapping. Note: *scale bars* are 23.00 μm

expression in the petal, pistil and seed and lower expression level in the root, stem and leaf (Fig. 7a). *LPAAT1* expression has not been previously reported in tree peony species, but its homolog expression has been observed in Arabidopsis with results similar to ours, as its expression was not restricted to typical oil storage organs such as seeds but was ubiquitous with low abundance [20].

The seed development process was observed from pollination until maturation. The pods of *P. rockii* were hand-collected at ten-day intervals from the 20 DAF until full maturity, covering a total range of 90 d, including S1, S2, S3, S4, S5, S6, S7, S8 and S9, a total of nine times. Figure 6a shows that the size and color varied dramatically at different stages of seed development. The fatty acid contents of seeds from nine developmental stages of *P. rockii* were characterized by GC–MS, and the FA content is depicted in Table S1. The results showed that five dominant components were found, namely, palmitic acid (C16:0, 5.6% of total FAs at S9), stearic acid (C18:0, 1.6%), oleic acid (C18:1Δ9c, 24.3%), linoleic acid (C18:2Δ9c, 12c, 26.1%), and α-linolenic acid (C18:3Δ9c, 12c, 15c, 41.7%). The combined content of these five FAs was more than 99.3% of total FAs at S9 and it was always predominant across the seed developmental stages, especially, the high proportion of n-3 FAs is quite rare in oil crops.

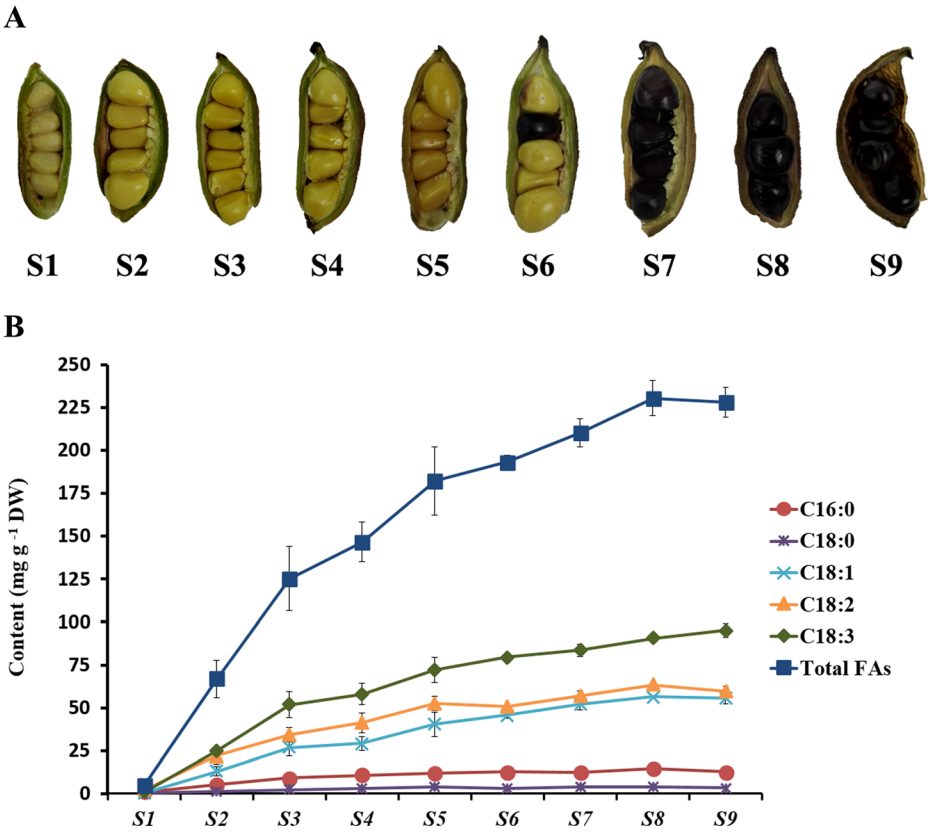

Fig. 6 Observation and measurement of lipids across the developmental period of tree peony seeds. **a** The developmental progress of *Paeonia rockii* seeds (S1–S9). The pods were harvested at 20 days after pollination (DAP, immature stage) and every 10 days thereafter until 100 DAP (pods containing mature seeds). **b** The total fatty acid content at five time points during tree peony seed development of *Paeonia rockii* (mean ± SD, $n = 3$)

Other minor FAs (<1.0%) were also detected including myristic acid (C14:0), palmitoleic acid (C16:1Δ9c), cis-11-octadecenoic acid (C18:1Δ11c), eicosanoic acid (C20:0) and cis-11-eicosenoic acid (C20:1Δ11c).

PrLPAAT1 gene expression was measured during seed development in the tree peony (Fig. 7b). The results demonstrated that *PrLPAAT1* expression had a biphasic pattern. *PrLPAAT1* exhibited relatively high transcript abundance during S1-S6 and dropped thereafter (S6-S9). The expression of the *PrLPAAT1* gene was increased at S1-S6, which coincided with the highest rate of FA accumulation in tree peony seeds (Fig. 6b). Interestingly, FA content was still increased at S6-S8, but *PrLPAAT1* exhibited relatively low transcript abundance at the same times. In conclusion, the expression of *PrLPAAT1* did not completely correlate with seed FA accumulation, especially during the late stages of seed development, such as the period from 70 to 100 DAF (S6-S9). However, these results indicated that *PrLPAAT1* is probably an

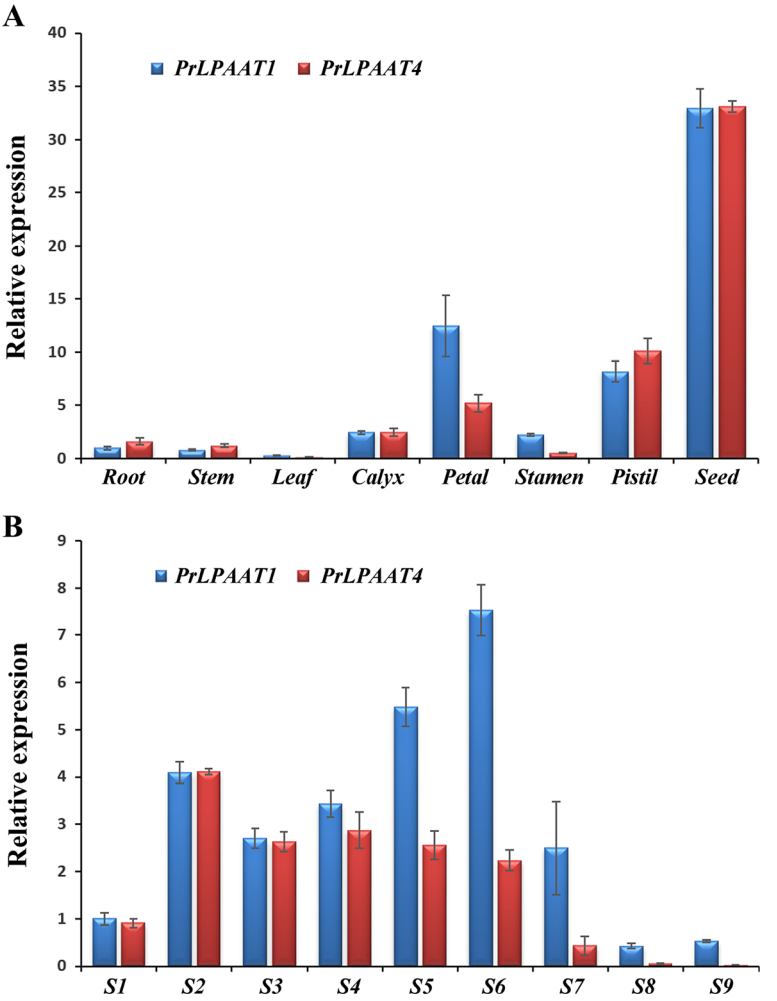

Fig. 7 Expression profile of the tree peony *PrLPAAT*s. **a** Tissue-specific expression of *PrLPAAT*s. **b** *PrLPAAT*s expression during tree peony seed development. Error bar represents the standard deviation of three replicates. The tree peony *18S RNA* was used as an internal control

important component of the lipid biosynthesis process, especially during the early stages of seed development.

Moreover, we have tried to clone other *PrLPAAT*s, but only *PrLPAAT4* was isolated from tree peony. In Fig. 7, the spatial and temporal expression of *PrLPAAT4* was measured. Analysis showed that the expression profile of *PrLPAAT4* was similar with that of *PrLPAAT1* in different tree peony organs and at S1-S4 stages of seed development. *PrLPAAT1* exhibited higher transcript abundances than *PrLPAAT4* during S5-S9. Similarly, the transcript abundances of *PrLPAAT1* and *PrLPAAT4* dropped markedly at S7-S9.

FA Levels in Mature *PrLPAAT1* Transgenic Arabidopsis Seeds

The FA content of mature seeds was measured in *PrLPAAT1* transgenic Arabidopsis lines by GC-MS. The total FA content increased by 19.37% in T1 overexpressing seeds compared with wild type (Fig. 7b). We wondered if that the change of total FAs content was based on the increase of one or more specific FAs, the FA profiles of seeds from wild type, and *PrLPAAT1* overexpression plants were analyzed (Fig. 7a). The results showed that most of the FAs have higher levels of production in the transgenic T1 seeds compared to wild type seeds, and the predominant FAs in the transgenic seeds were C18:1, C18:2, C18:3, C20:1, and C16:0 (Fig. 8).

Discussion

In recent years, the tree peony has been found to be an excellent woody oil crop with a have high oil production rate and good oil quality. As an alternative source of edible oil, the tree peony could be sustainably exploited, and it is a good model for dissecting the metabolic pathways involved in seed oil synthesis. Currently, tree peony genetic engineering is an emerging field, and the cloning and functional analysis of genes related to fatty acid metabolism have not yet been reported. In this study, we cloned and identified one *LPAAT* gene encoding a LPAAT-like protein from the tree peony known as *PrLPAAT1*. The full-length cDNA fragment harbored a 1047 bp ORF encoding a 348-aa peptide, and the *PrLPAAT1* gene did not contain introns. Like most plant species (with the exception of *G. max*), the tree peony harbored a single *LPAAT1* gene. The subcellular localization of PrLPAAT1 was analyzed in the tree peony. Inspection of the subcellular localization of PrLPAAT1 in the lower epidermis cells

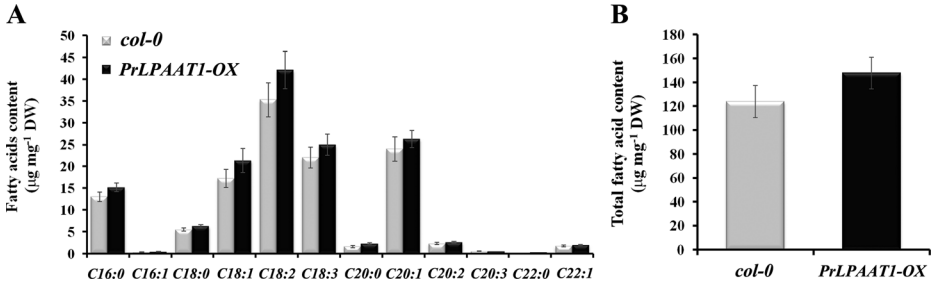

Fig. 8 Effect of *PrLPAAT1* overexpression on FA content in Arabidopsis seeds. **a** FA profiles of wild type (Col-0) and *PrLPAAT1*-overexpressing (*PrLPAAT1*-OX) plants. **b** Total fatty acid content of Col-0 and *PrLPAAT1*-OX plants

of tobacco leaves revealed that this protein is concentrated on membrane structures (Fig. 5), and these results indicated that PrLPAAT1 was a plasma membrane protein, which was not consistent with previous studies in Arabidopsis [51]. The Arabidopsis LPAAT1 protein (ATS2) is localized in the plastid. As shown in Fig. 5, the tree peony PrLPAAT1 protein may also be localized in the plastid, but this is not very obvious.

LPAATs play an important role in the lipid metabolism of living organisms [19]. To explore the evolutionary history of the *LPAAT1*s, the newly published genomes of several species were used, including algae, angiosperms and metazoan animals. Based on the previous researches, our work predicted the evolutionary relationships of *LPAAT1*s in species and elucidated the contribution of *PrLPAAT1* during evolution. We identified that the *LPAAT1*s could encode the enzymes which are catalyzing the second acylation reaction of TAG assembly in several species. Two primary clusters were exhibited in the phylogenetic tree (animals and plants). Our phylogenetic analyses showed that *LPAAT1* genes emerged early and were transmitted vertically and horizontally during the eukaryotic evolution. Plant *LPAAT1*s and animal *AGPAT1/2* s (Fig. 3) are related to the prokaryotic *LPAAT*s compactly. Moreover, PrLPAAT1 shared 74.3 and 65.5% amino acid sequence identities with those from columbine and grape, respectively, suggesting that these genes might play similar roles in lipid metabolism.

The relatively high conservation of gene structure was observed between genes in the same cluster by phylogenetic reconstruction, which was considered in an ancient gene family that play an important role in virtually all livings. Interestingly, the tree peony *LPAAT1* gene did not contain any intron sequences (Fig. 4a), which is very rare in eukaryote *LPAAT1* genes. The results suggested that these genes would be activated at the later diversification events during the eukaryotic evolution. The integration of previous studies [19, 22, 51] with the present results supports the hypothesis that *LPAAT1* genes have different origins in species during the eukaryote evolution. *LPAAT1* could be observed in all studied species, and it is a plastidic isoform that is participated in the production of PA with C16 FAs at the sn-2 position, which is similar to the prokaryotic formation, all of that redouble supported our phylogenetic tree analysis. Predictions of transmembrane (TrM) structures suggested that each *PrLPAAT1* gene has at least two regions which contained an extremely probable TrM sequence (Fig. 4b), which indicated that the PrLPAAT1 protein is associated with membrane systems, which was confirmed by subcellular localization analysis (Fig. 5).

From qRT-PCR analyses, it was shown that *PrLPAAT1* was expressed constitutively, although this expression was low in the root, stem and leaf. These findings were consistent with the previous studies in Arabidopsis, in which expression of *AtLPAAT1* [51] was detected constitutively. Thus, we proposed that *PrLPAAT1* might be involved in the production of PA for a constitutive requirement in most tissues. Our study showed that *PrLPAAT1* expression was higher in the flower and developing seed than that in vegetative organs (root, stem and leaf). In contrast, *LPAAT1* in Arabidopsis had a distinct tissue distribution, with higher expression in the leaf, stem, flower, and developing seed (4 days after flowering) and lower expression in the root [51]. Interestingly, *PrLPAAT1* expression was higher in the petal and pistil than in the calyx and stamen, suggesting that *PrLPAAT1* might play different roles in different parts of the flower.

Our results showed that FAs in *Paeonia rockii* mainly included palmitic acid (C16:0, PA), stearic acid (C18:0, SA), oleic acid (C18:1Δ9c, OA), linoleic acid (C18:2Δ9c, 12c, LA), and α-linolenic acid (C18:3Δ9c, 12c, 15c, ALA), the content of five dominant FAs steadily increased during seed development (Fig. 6b). The expression of *PrLPAAT1* was detected at

all stages of seed development (20 DAF to maturity). Furthermore, *PrLPAAT1* expression was increased at S1-S6 (Fig. 7b), which coincided with the highest rate of FA accumulation in tree peony seeds (Fig. 6b). These results indicated that *PrLPAAT1* is probably an important component in the FA accumulation process (or Kennedy pathway), especially during the early stages of seed development. Furthermore,*Paeonia rockii* seed oil contains >90% unsaturated C18s, it cannot be excluded that PC-derived pathways contributed to the TAG synthesis [52]. PC is an intermediate in the flux of FAs or diacylglycerol, or both substrates into TAG [11], and its sn-2 position is the main site of FA modification [53, 54]. The process of Acyl fluxes into and out of PC is significant for the production of TAG containing high amounts of the polyunsaturated FAs (PUFA) [55]. From a single Kennedy pathway to >90% PC-derived pathways, the pathway of TAG synthesis appears to differ in plants [11]. Interestingly, The FA content increased at S6-S8, but the *PrLPAAT*s exhibited relatively low transcript abundance at the same times. In this scenario, we speculate that PC-derived pathways played a major role in the TAG synthesis during the late stages of seed development.

PrLPAAT1 overexpression using a seed-specific promoter increased total FA content and the main FA accumulation in Arabidopsis transgenic plants. These results suggested that *PrLPAAT1* plays an important role in tree peony FA accumulation.

Conclusions

In conclusion, we cloned the Lysophosphatidic acid acyltransferase gene *PrLPAAT1* from *Paeonia rockii*, and using bioinformatics analysis, we confirmed that the *PrLPAAT1* was highly homologous with the characterized *LPAAT* from columbine and grape. Subcellular localization analysis confirmed that PrLPAAT1 was a plasma membrane protein. *PrLPAAT1* was ubiquitously expressed in diverse tissues, and it was more highly expressed in the developing seed. At 20–60 DAF, *PrLPAAT1* expression was increased and coincided with the highest rate of FA accumulation. The total FA content and the main FA accumulation were increased by using a seed-specific promoter to overexpress the *PrLPAAT1* in Arabidopsis transgenic plants. These results indicated that *PrLPAAT1* probably plays an important role in tree peony FA accumulation and TAG assembly.

Acknowledgements This work was financially supported by the National Forestry Public Welfare Industry Research Project of China (201404701).

Compliance with Ethical Standards

Conflict of Interest The authors declare no conflict of interest.

References

1. Yuan, J. H., Cheng, F. Y., & Zhou, S. L. (2011). The phylogeographic structure and conservation genetics of the endangered tree peony, *Paeonia rockii* (Paeoniaceae), inferred from chloroplast gene sequences. *Conservation Genetics, 12*, 1539–1549.
2. Hong, D. Y., & Pan, K. Y. (2005). Notes on taxonomy of *Paeonia* sect. *Moutan* DC. (Paeoniaceae). *Acta Phytotaxonomica Sinica, 43*, 169–177.

3. Simopoulos, A. P. (2002). The importance of the ratio of omega-6/omega-3 essential fatty acids. *Biomedicine and Pharmacotherapy, 56*, 365–379.
4. Simopoulos, A. P. (2006). Evolutionary aspects of diet, the omega-6/omega-3 ratio and genetic variation: nutritional implications for chronic diseases. *Biomedicine and Pharmacotherapy, 60*, 502–507.
5. Li, S. S., Yuan, R. Y., Chen, L. G., Wang, L. S., Hao, X. H., Wang, L. J., Zheng, X. C., & Du, H. (2015). Systematic qualitative and quantitative assessment of fatty acids in the seeds of 60 tree peony (*Paeonia* section *Moutan* DC.) cultivars by GC-MS. *Food Chemistry, 173*, 133–140.
6. Zhang, M., Fan, J., Taylor, D. C., & Ohlrogge, J. B. (2009). Dgat1 and pdat1 acyltransferases have overlapping functions in *Arabidopsis* triacylglycerol biosynthesis and are essential for normal pollen and seed development. *Plant Cell, 21*, 3885–3901.
7. Li-Beisson, Y., Shorrosh, B., Beisson, F., Andersson, M. X., Arondel, V., Bates, P. D., Baud, S., Bird, D., DeBono, A., Durrett, T. P., Franke, R. B., Graham, I. A., Katayama, K., Kelly, A. A., Larson, T., Markham, J. E., Miquel, M., Molina, I., Nishida, I., Rowland, O., Samuels, L., Schmid, K. M., Wada, H., Welti, R., Xu, C., Zallot, R., & Ohlrogge, J. (2013). Acyl-lipid metabolism. *The Arabidopsis Book/American Society of Plant Biologists, 11* .e0161
8. Yuan, Y., Liang, Y., Gao, L., Sun, R., Zheng, Y., & Li, D. (2015). Functional heterologous expression of a lysophosphatidic acid acyltransferase from coconut (*Cocos nucifera* L.) endosperm in *Saccharomyces cerevisiae* and *Nicotiana tabacum*. *Scientia Horticulturae, 192*, 224–230.
9. Durrett, T. P., Benning, C., & Ohlrogge, J. (2008). Plant triacylglycerols as feedstocks for the production of biofuels. *Plant Journal, 54*, 593–607.
10. Dyer, J. M., Stymne, S., Green, A. G., & Carlsson, A. S. (2008). High-value oils from plants. *Plant Journal, 54*, 640–655.
11. Bates, P. D., & Browse, J. (2012). The significance of different diacylgycerol synthesis pathways on plant oil composition and bioengineering. *Frontiers in Plant Science, 3*, 147.
12. Chapman, K. D., & Ohlrogge, J. B. (2012). Compartmentation of triacylglycerol accumulation in plants. *Journal of Biological Chemistry, 287*, 2288–2294.
13. Chen, S., Lei, Y., Xu, X., Huang, J., Jiang, H., Wang, J., Cheng, Z., Zhang, J., Song, Y., Liao, B., & Li, Y. (2015). The peanut (*Arachis hypogaea* L.) Gene *AhLPAT2* increases the lipid content of transgenic Arabidopsis seeds. *PloS One, 10* .e0136170
14. Li-Beisson, Y., Shorrosh, B., Beisson, F., Andersson, M. X., Arondel, V., Bates, P. D., Baud, S., Bird, D., Debono, A., Durrett, T. P., Franke, R. B., Graham, I. A., Katayama, K., Kelly, A. A., Larson, T., Markham, J. E., Miquel, M., Molina, I., Nishida, I., Rowland, O., Samuels, L., Schmid, K. M., Wada, H., Welti, R., Xu, C., Zallot, R., Ohlrogge, J. (2013). Acyllipid metabolism. Arabidopsis Book, 11, e0161.
15. Dahlqvist, A., Stahl, U., Lenman, M., Banas, A., Lee, M., Sandager, L., Ronne, H., & Stymne, S. (2000). Phospholipid: diacylglycerol acyltransferase: an enzyme that catalyzes the acyl-CoA-independent formation of triacylglycerol in yeast and plants. *Proceedings of the National Academy of Sciences, 97*, 6487–6492.
16. Lee, K. R., Chen, G. Q., & Kim, H. U. (2015). Current progress towards the metabolic engineering of plant seed oil for hydroxy fatty acids production. *Plant Cell Reports, 34*, 603–615.
17. Agarwal, A. K. (2012). Lysophospholipid acyltransferases: 1-acylglycerol-3-phosphate O-acyltransferases. From discovery to disease. *Current Opinion in Lipidology, 23*, 290–302.
18. Coleman, R. A., & Lee, D. P. (2004). Enzymes of triacylglycerol synthesis and their regulation. *Progress in Lipid Research, 43*, 134–176.
19. Körbes, A. P., Kulcheski, F. R., Margis, R., Margis-Pinheiro, M., & Turchetto-Zolet, A. C. (2016). Molecular evolution of the lysophosphatidic acid acyltransferase (LPAAT) gene family. *Molecular Phylogenetics and Evolution, 96*, 55–69.
20. Kim, H. U., Li, Y., & Huang, A. H. (2005). Ubiquitous and endoplasmic reticulum-located lysophosphatidyl acyltransferase, LPAT2, is essential for female but not male gametophyte development in Arabidopsis. *Plant Cell, 17*, 1073–1089.
21. Roscoe, T. J. (2005). Identification of acyltransferases controlling triacylglycerol biosynthesis in oilseeds using a genomics-based approach. *European Journal of Lipid Science and Technology, 107*, 256–262.
22. Arroyo-Caro, J. M., Chileh, T., Kazachkov, M., Zou, J., Alonso, D. L., & García-Maroto, F. (2013). The multigene family of lysophosphatidate acyltransferase (LPAT)-related enzymes in *Ricinus communis*: cloning and molecular characterization of two *LPAT* genes that are expressed in castor seeds. *Plant Science, 199–200*, 29–40.
23. Brown, A., Brough, C., Kroon, J., & Slabas, A. (1995). Identification of a cDNA that encodes a 1-acyl-sn-glycerol-3-phosphate acyltransferase from *Limnanthes douglasii*. *Plant Molecular Biology, 29*, 267–278.
24. Hanke, C., Wolter, F. P., Coleman, J., Peterek, G., & Frentzen, M. (1995). A plant acyltransferase involved in triacylglycerol biosynthesis complements an *Escherichia coli* sn-1-acylglycerol-3-phosphate acyltransferase mutant. *European Journal of Biochemistry, 232*, 806–810.

25. Knutzon, D. S., Lardizabal, K. D., Nelsen, J. S., Bleibaum, J. L., Davies, H. M., & Metz, J. G. (1995). Cloning of a coconut endosperm cDNA encoding a 1-acyl-sn-glycerol-3-phosphate acyltransferase that accepts medium-chain-length substrates. *Plant Physiology, 109*, 999–1006.
26. Yu, X. H., Prakash, R. R., Sweet, M., & Shanklin, J. (2014). Coexpressing *Escherichia coli* cyclopropane synthase with *Sterculia foetida* lysophosphatidic acid acyltransferase enhances cyclopropane fatty acid accumulation. *Plant Physiology, 164*, 455–465.
27. Chen, G. Q., van Erp, H., Martin-Moreno, J., Johnson, K., Morales, E., Browse, J., Eastmond, P. J., & Lin, J. T. (2016). Expression of Castor LPAT2 enhances ricinoleic acid content at the sn-2 position of triacylglycerols in Lesquerella seed. *International Journal of Molecular Sciences, 17*, 507.
28. Maisonneuve, S., Bessoule, J. J., Lessire, R., Delseny, M., & Roscoe, T. J. (2010). Expression of rapeseed microsomal lysophosphatidic acid acyltransferase isozymes enhances seed oil content in Arabidopsis. *Plant Physiology, 152*, 670–684.
29. Chen, S. L., Huang, J. Q., Lei, Y., Zhang, Y. T., Ren, X. P., Chen, Y. N., Jiang, H. F., Yan, L. Y., Li, Y. R., & Liao, B. S. (2012). Identification and characterization of a gene encoding a putative lysophosphatidyl acyltransferase from *Arachis hypogaea*. *Journal of Biosciences, 37*, 1029–1039.
30. Zou, J., Katavic, V., Giblin, E. M., Barton, D. L., MacKenzie, S. L., Keller, W. A., Hu, X., & Taylor, D. C. (1997). Modification of seed oil content and acyl composition in the brassicaceae by expression of a yeast sn-2 acyltransferase gene. *Plant Cell, 9*, 909–923.
31. Rao, S. S., & Hildebrand, D. (2009). Changes in oil content of transgenic soybeans expressing the yeast *SLC1* gene. *Lipids, 44*, 945–951.
32. Kim, H. U., & Huang, A. H. C. (2004). Plastid lysophosphatidyl acyltransferase is essential for embryo development in Arabidopsis. *Plant Physiology, 134*, 1206–1216.
33. Wallis, J. G., & Browse, J. (2010). Lipid biochemists salute the genome. *Plant Journal, 16*, 1092–1106.
34. Gao, Q., Lu, Y., Yao, H., Xu, Y. J., Huang, W., & Wang, C. (2016). Phospholipid homeostasis maintains cell polarity, development and virulence in *metarhizium robertsii*. *Environmental Microbiology*. doi:10.1111/1462-2920.13408.
35. Allen, G. C., Flores-Vergara, M. A., Krasynanski, S., Kumar, S., & Thompson, W. F. (2006). A modified protocol for rapid DNA isolation from plant tissues using cetyltrimethylammonium bromide. *Nature Protocols, 1*, 2320–2325.
36. Kelley, L. A., & Sternberg, M. J. (2009). Protein structure prediction on the web: a case study using the Phyre server. *Nature Protocols, 4*, 363–371.
37. Larkin, M. A., Blackshields, G., Brown, N. P., Chenna, R., McGettigan, P. A., McWilliam, H., Valentin, F., Wallace, I. M., Wilm, A., Lopez, R., Thompson, J. D., Gibson, T. J., & Hiqqins, D. G. (2007). Clustal W and Clustal X version 2.0. *Bioinformatics, 23*, 2947–2948.
38. Saitou, N., & Nei, M. (1987). The neighbor-joining method: a new method for reconstructing phylogenetic trees. *Molecular Biology and Evolution, 4*, 406–425.
39. Tamura, K., Peterson, D., Peterson, N., Stecher, G., Nei, M., & Kumar, S. (2011). MEGA5: molecular evolutionary genetics analysis using maximum likelihood, evolutionary distance, and maximum parsimony methods. *Molecular Biology and Evolution, 28*, 2731–2739.
40. Rambaldi, D., & Ciccarelli, F. D. (2009). FancyGene: dynamic visualization of gene structures and protein domain architectures on genomic loci. *Bioinformatics, 25*, 2281–2282.
41. Clough, S. J., & Bent, A. F. (1998). Floral dip: a simplified method for agrobacterium mediated transformation of *Arabidopsis thaliana*. *Plant Journal, 16*, 735–743.
42. Yamashita, A., Hayashi, Y., Matsumoto, N., Nemoto-Sasaki, Y., Oka, S., Tanikawa, T., & Sugiura, T. (2014). Glycerophosphate/Acylglycerophosphate acyltransferases. *Biology, 3*, 801–830.
43. Lewin, T. M., Wang, P., & Coleman, R. A. (1999). Analysis of amino acid motifs diagnostic for the sn-glycerol-3-phosphate acyltransferase reaction. *Biochemistry, 38*, 5764–5771.
44. Ghosh, A. K., Ramakrishnan, G., Chandramohan, C., & Rajasekharan, R. (2008). CGI-58, the causative gene for Chanarin-Dorfman syndrome, mediates acylation of lysophosphatidic acid. *Journal of Biological Chemistry, 283*, 24525–24533.
45. Yamashita, A., Nakanishi, H., Suzuki, H., Kamata, R., Tanaka, K., Waku, K., & Sugiura, T. (2007). Topology of acyltransferase motifs and substrate specificity and accessibility in 1-acyl-sn-glycero-3-phosphate acyltransferase 1. *Biochimica et Biophysica Acta, 1771*, 1202–1215.
46. Harayama, T., Shindou, H., Ogasawara, R., Suwabe, A., & Shimizu, T. (2008). Identification of a novel noninflammatory biosynthetic pathway of platelet-activating factor. *Journal of Biological Chemistry, 283*, 11097–11106.
47. Albesa-Jove, D., Svetlikova, Z., Tersa, M., Sancho-Vaello, E., Carreras-Gonzalez, A., Bonnet, P., Arrasate, P., Eguskiza, A., Angala, S. K., Cifuente, J. O., Kordulakova, J., Jackson, M., Mikusova, K., & Guerin, M. E. (2016). Structural basis for selective recognition of acyl chains by the membrane-associated acyltransferase PatA. *Nature Communications, 7*, 10906–10906.

48. Tamada, T., Feese, M. D., Ferri, S. R., Kato, Y., Yajima, R., Toguri, T., & Kuroki, R. (2004). Substrate recognition and selectivity of plant glycerol-3-phosphate acyltransferases (GPATs) from Cucurbita moscata and Spinacea oleracea. *Acta Crystallographica, 60*, 13–21.
49. Agarwal, A. K., Sukumaran, S., Cortés, V. A., Tunison, K., Mizrachi, D., Sankella, S., Gerard, R. D., Horton, J. D., & Garg, A. (2011). Human 1-acylglycerol-3-phosphate Oacyltransferase isoforms 1 and 2: biochemical characterization and inability to rescue hepatic steatosis in Agpat2(−/−) gene lipodystrophic mice. *Journal of Biological Chemistry, 286*, 37676–37691.
50. Wang, Y., You, F. M., Lazo, G. R., Luo, M. C., Thilmony, R., Gordon, S., Kianian, S. F., & Gu, Y. K. (2013). PIECE: a database for plant gene structure comparison and evolution. *Nucleic Acids Research, 41*.
51. Yu, B., Wakao, S., Fan, J., & Benning, C. (2004). Loss of plastidic lysophosphatidic acid acyltransferase causes embryo-lethality in *Arabidopsis*. *Plant and Cell Physiology, 45*, 503–510.
52. Bates, P. D., Stymne, S., & Ohlrogge, J. (2013). Biochemical pathways in seed oil synthesis. *Current Opinion in Plant Biology, 16*, 358–364.
53. Sperling, P., Linscheid, M., Stocker, S., Muhlbach, H. P., & Heinz, E. (1993). In vivo desaturation of cis-delta-9-monounsaturated to cis-delta-9, 12-diunsaturated alkenylether glycerolipids. *Journal of Biological Chemistry, 268*, 26935–26940.
54. Vandeloo, F. J., Broun, P., Turner, S., & Somerville, C. (1995). An oleate 12-hydroxylase from Ricinus communis L. is a fatty acyl desaturase homolog. *Proceedings of the National Academy of Sciences, 92*, 6743–6747.
55. Wallis, J. G., Watts, J. L., & Browse, J. (2002). Polyunsaturated fatty acid synthesis: what will they think of next? *Trends in Biochemical Sciences, 27*, 467–473.